Magnetic Separation News, Vol. 2, pp. 155–175
Reprints available directly from the publisher
Photocopying permitted by license only

MATHEMATICAL AND EXPERIMENTAL MODELLING OF HIGH-GRADIENT MAGNETIC SEPARATION ON ROD MATRICES

KAREL JAHODA AND VLADIMIR HENCL
Czechoslovak Academy of Sciences, Institute of Geology and Geotechnics, 182 09 Prague 8,
V Holesovickach 41, Czechoslovakia.

ABSTRACT The use of new mathematical and experimental modelling of the HGMS process is described. Mathematical modelling, complemented by some experimentally determined values, was found to permit the determination, with a high reliability, of process parameters, even for industrial-scale conditions.

INTRODUCTION

Results of the experimental research of magnetic separation in high-gradient magnetic separators with oriented rod matrices revealed that some of the present ideas about the course of the separation will have to be replaced by other hypotheses. /1/ The discussed mathematical model embodies three new hypotheses according to which:

(1) Magnetic particles from a suspension need not to be attracted to the rods, being carried to them by the suspension and the magnetic attractive force prevents them from being washed away.

(2) The limit layer of entrapped particles is determined by lines of force or by equipotential lines of the magnetic field between the rods; they cannot be determined from flow conditions only.

(3) The maximum size of particles that can still be kept by the magnetizable surface of the rods in a trapped layer has to be determined not from the dynamical but from the suction effect of the flowing suspension.

Theoretical calculations based on these hypotheses provided a

satisfactory fit with laboratory and industrial-scale experiments. They were therefore incorporated into the mathematical model. Equations of this model are presented in their basic form. Iteration computation method enables the non-homogeneity of the feed, which represents a mixture of particles of various sizes and contents of the magnetic component, to be taken in account. Output of the mathematical model yielded some interesting data. One of them, concerning the application of laboratory measurements to operating conditions, is discussed in a separate chapter.

THE EQUATIONS OF THE MATHEMATICAL MODEL

Passage of particles through a matrix

During suspension flow through a matrix, the particles can be entrapped only on sufficiently magnetized surfaces of rods, usually about in the centre of the rod circumference. The area of a possible retaining of particles lies within the angle $2\phi = 90°$ (Fig. 1a). As the figure shows, this area involves a part of the cross-sectional flow area according to the equation:

$$p = 2R\sin\phi / T \qquad (1)$$

For a uniform dispersion of particles in the suspension, the value of p represents the probability that a certain particle will be carried to the magnetized surface of the rod. It is probable that, the suspension passes through n rows of rods, during this passage the particle can generally be carried x times to the magnetized part of the surface. As known from statistics, the probability p (x) of such a phenomenon is given by the expression for binomial distribution.

$$p\,(x) = \binom{n}{x}\, p^{x}\,(1-p)^{n-x}$$

It follows that the particle will be carried to the magnetizable part with probability P (1) at least once, when

$$P\,(1) = 1 - (1-p)^{n} \qquad (2)$$

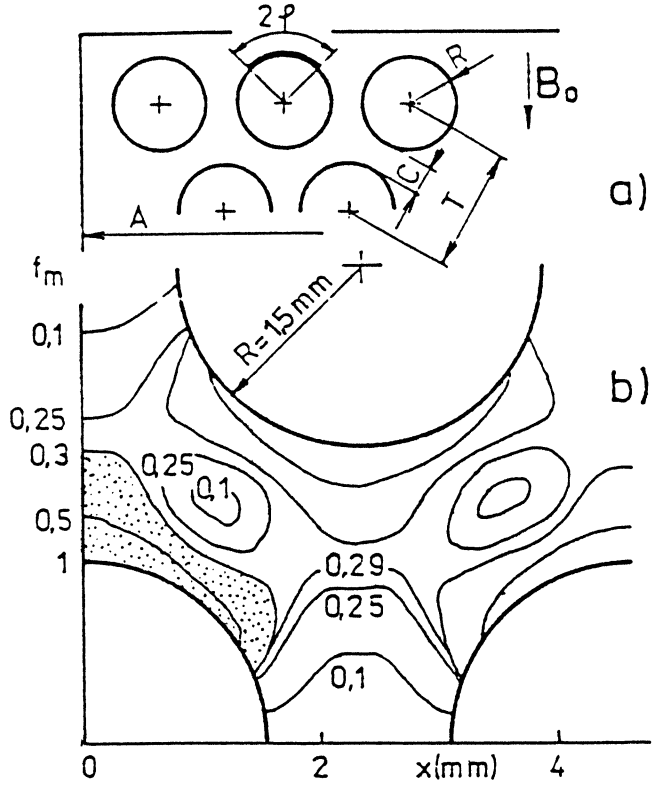

FIGURE 1. a) arrangement of inductive rods in a matrix
b) field of force between rods

For values from Fig. 1, p = 0.386; if the suspension flows through n = 32 rows of rods, (height of matrix 150 mm) P (1) = 99.99998%. The number of particles in the suspension is so high that the laws of statistics can be applied with nearly absolute reliability. This results also in the first of our hypotheses: the particles are carried to the magnetized part of the surface by the suspension flow and they need not to be attracted to it.

The carry-along forces of the flow

The flow in the matrix is rather slow, about 0.1 m/s for most of the mineral raw materials. Assessed according to Reynold's number, this flow should be laminar, namely for flowing around entrapped particles. A laminar flow is characterized primarily by the translation motion of both the particles and the liquid. This condition cannot be practically fulfilled as the flow among inductive rods is subjected to repeated tapering and expansion of the cross-sectional area. Also, a multiple change of the flow direction occurs during by-passing of these rods. This causes a disarranged motion of particles and liquid, i.e., turbulent flow. The carrying effect of such a flow is quite satisfactorily explained by means of mean volume velocity v; the carrying force of flow, referred to a unit mass of a particle, is computed from the relation

$$f_e = \frac{v^2}{2} \frac{3\rho}{2\rho_z d_i} \qquad (N\,kg^{-1})$$

$$\xi = 1 + 18.5\,\psi\,Re^{0.6},\ Re = v\,d_i/\nu \qquad (3)$$

ξ is the hydraulic resistance coefficient and ψ reflects which part of the particle cross-section is directly exposed to the flow effect. Should the particles be attracted to the rods, the attracting force would have to overcome the resistance of the whole particle cross-section when $\psi = 1$. A particle brought by the flow to the layer of already caught particles may be entirely embodied in this layer, when $\psi = 0$, or protrude from it entirely when $\psi = 1$. The statistically most probable case is $\psi = 0.5$.

Attracting forces in a matrix

Equations, defining the magnetic potential in the rod matrix /2/, could be used to define the field of force in this matrix /2/. Fig. 1b shows contour lines ϕ m, connecting places in which the particles are affected by the same specific attractive force, referred to its maximum value in point F. The relevant equations are too extensive for being quoted here /3/; the figure shows the outputs from the HP 9830 B computer for a certain specific case. The attracting force acting in the z axis and referred again to the unit mass of particle can be quite precisely determined from the formula

$$f_m = \frac{4\chi B_o^2 R^3}{\mu_o R \quad z^3} \quad (N\ kg^{-1}) \qquad (4)$$

It is evident from Fig. 2 this equation holds exactly up to the value of z/R = 1.5; a technical calculation z/R = 1.2-1.4, is mostly used. The attracting and carrying forces on the boundary layer must be in equilibrium $f_m = f_e$. The carrying force of a turbulent flow can be regarded, in first approximation, as constant. In such a case, the boundaries of the layers of entrapped particles are formed by contour lines f_m = const. This is the basis of the second hypothesis. Fig. 1b indicates a contour line f_m =0.3, the last one closed on the surface of the same rod. Contour line 0.29 is already closed between the surfaces of two adjacent rods; at high values of B_o and χ, flow could be clogged. The area defined by the contour line f_m = 0.3 (marked by dotting) has the surface $S = 0.6\ \Pi\ R^2$. This practically determines the maximum mass of particles which can be trapped in a matrix during the flow. This mass, referred to the unit of matrix volume, reflects its specific capacity m_o, given by

$$m_o = \frac{2}{\sqrt{3}\ T^2}\ 0.6\Pi\ R^2\ \rho_{zs} \quad (kg\ m^{-3}) \qquad (5)$$

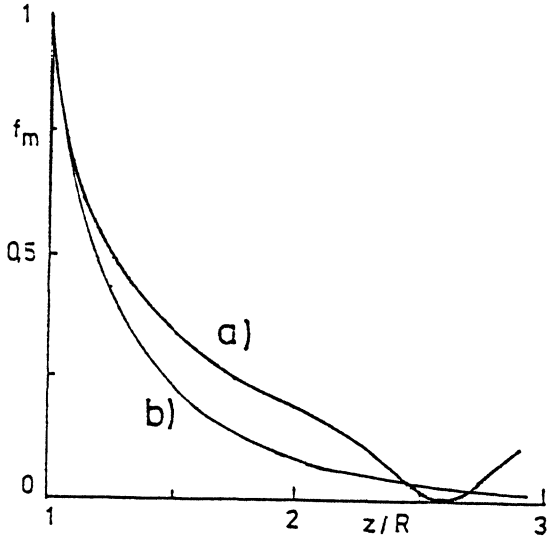

FIGURE 2. Decrease of the specific attractive force f_m with the distance.
a) obtained by precise calculation.
b) obtained by approximate calculation from the equation (4).

Limit size of particles

In a limit case the particle can be entirely embedded in the layer being formed of trapped particles and can only be washed out into the flowing suspension by means of the suction effect of the flow. A particle completely embedded in the layer is not exposed to direct effects of the flow and in this case, $\psi = 0$ is inserted

into equation (3). It is also evident, from this equation, that the drifting effect of the flow f_e on the particle is higher the smaller is the particle. The smallest particles can be trapped near the surface, where $z \doteq R$ and where the attractive force is the greatest (equation 4). From the equilibirum condition $f_m = f_e$, the expression for calculation of a specific particle size is obtained:

$$d_e = \frac{v^2}{2} \quad \frac{3\rho}{2\rho_z} \quad \frac{\mu_o R}{4\chi B_o^2} \qquad (m) \qquad (6)$$

The separation yield can also include a small proportion of particles much smaller, including those non-magnetic carried into the layer mechanically together with larger particles and entrapped there.

Input values of the model

The input values presented here hold for a sideroplessite ore from Rudnany (siderite with isomorphic Fe instead of Mn, Mg, Ca) containing 25.17% Fe. Values of metal Fe content and yield (recovery) used in the model are expressed as fractions of number one-it simplifies to a great extent the computations, mathematical operations and the formulation of final equations. Input values expressing the properties of the charge are illustrated in Fig. 3. They are: basic diagram of the dressing ability (Fig. 3a), dependence of the specific magnetic susceptibility χ on the metal Fe content of the ore β, and the dependence of the screen oversizes yield on the size of the particles. The inputs used in computing have the following numerical values:

$\alpha = 0.2517$ - Fe content in the charge

$\beta_s = 0.4062$ - Fe content in the pure sideroplessite from Rudnany

$\chi = 84.10^{-8}\ m^3/kg$ - specific magnetic susceptibility at $\beta_i \doteq 0.22$ - Fig. 3b

ρ_z = 3400 kg/m^3 - specific mass of magnetic particles.
ρ_{zs} = 2300 kg/m^3 - bulk mass of particles.
ρ_s = 500 kg/m^3 - suspension density-particles mass in the unit of suspension volume.
d = 67 . 10^{-6} m- particles mean size.
R = 0.0015 m - radius of inductive rods.
T = 0.0045 m - rods spacing.
η_o = 4 . 10^{-7} H/m- permeability of vacuum.
B_o = 0.5 T - background magnetic field.
ρ = 1000 kg/m^3 - specific mass of water.
ν = 10^{-6} m^2/s - kinematic viscosity of water.
m_o = 556 kg/m^3 - specific capacity of the matrix.
m = 500 kg/m^3 - specific matrix loading i.e. mass of particles in one dose of the suspension related to the volume unit of matrix.
v = 0.146 m/s - mean volume velocity of suspension flowing in gaps between inductive rods.

Calculations

These include mainly the calculation of the yield γ and recovery of Fe concentrate. The method of calculation is substantially a mathematical expression of the course of the separation process. The first layer of particles is entrapped directly on the surface of the inductive rods. Further particles are trapped on this layer, etc. Let a case when the first layer is formed by particles trapped from a small dose of suspension, containing d_m = 50 kg/m^3 of particles, be considered. A small part of this amount $d\gamma_i$ = 0.1 has the metal content β_i = 0.22 i.e., the specific magnetic susceptibility χ_i = 84.10^{-8} m^3/kg (Fig. 3a, 3b). The condition of dynamic equilibrium $f_m = f_e$ implies that the carrying effect of the flow will remove all particles, smaller than d_i

$$d_i \doteq \left[\frac{12\nu^{0.6} v^{1.4} 3\rho}{4\rho_z} \quad \frac{\mu_o R}{4 \chi B_o^2} \frac{z^3}{R^3} \right]^{0.625} (m) \qquad (7)$$

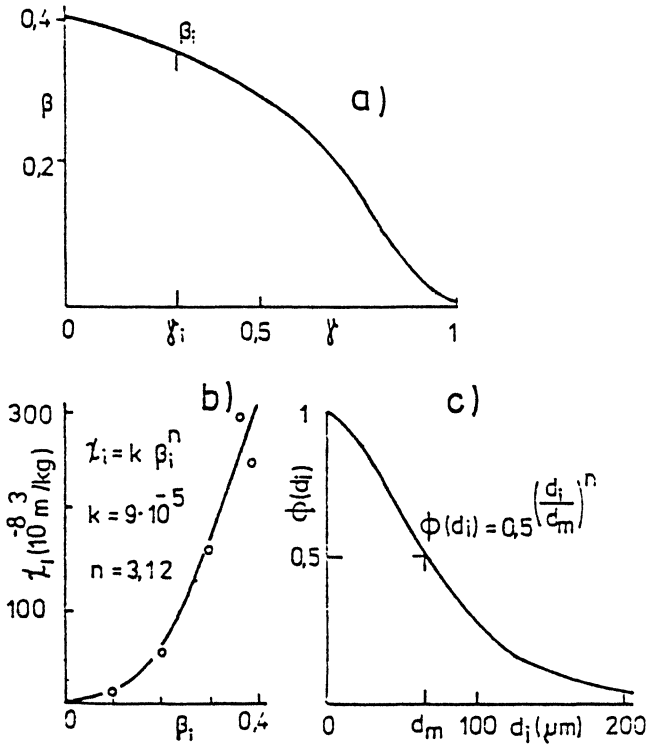

FIGURE 3. Dependence of

a) metal content β_i on the yield for ideal particles arrangement.

b) magnetic susceptibility χ on metal content of particles in the feed.

c) screen oversizes yield on particle size.

A more precise value would be obtained from equations (3) and (4), using some of the iterative numerical methods. As already mentioned in equation (3), the coefficient Ψ is assumed to equal 0.5. By introducing the assigned input values, it can be established that all particles smaller than $d_i \doteq 43 \cdot 10^{-6}$ m will be carried away at z = R. This will reduce the yield in this class of metal content β_i to $\Phi(d_i)=0.7$ (Fig.3c) of the ideal yield,

i.e. to the value of $\Phi(d_i)\, d\gamma = 0.07$. This recovery will contain $\beta_i\, \Phi(d_i)\, d\gamma = 0.0154$ parts of metal.

By effecting these calculations for all 10 intervals we obtain for the yield of the first layer

$$\gamma_1 = \sum_{i=1}^{i=10} \phi(d_i)\, d\gamma_i = 0.69$$

In the first layer, $\gamma_1 dm = 34.5$ kg/m^3 particles will be trapped on the rods. The cross-section S of the layer of trapped particles relative to the cross-section of rods is

$$\frac{S}{\pi R^2} = \gamma_i\, dm\, \frac{T^2\sqrt{3}}{2\pi R^2 \rho_{zs}}$$

By substitution, $S/\pi R^2 = 0.0372$ is obtained; a corresponding value of $z/R = 1.065$ is found from the graph in Fig.4 . This diagram expresses the relationship between the maximum thickness and the cross-sectional area of the layer of trapped particles. The corresponding contour line connecting places of the same specific magnetic attractive force determines the limit of every layer. Fig. 4 was obtained by numerical integration for this special case but it holds true for all $T/R > 2.5$. When calculating the yield (recovery) from the second part of the dose the procedure is equal, the previously computed value of $z/R = 1.065$ being substituted in the equations (4) or (7). This value reveals that particles from the second dose of suspension start to be trapped on the first layer, i.e. at a certain distance from the surface of the rod (where the attractive force is smaller). Therefore also the calculated yield $\gamma_2 \doteq 0.68$ is somewhat smaller and $\gamma_2\, dm = 34$ kg/m^3 of particles will be fixed on the rods in the second layer. We may compute, from the previous equation, that $S/\pi R^2 = 0.0739$. We find now in Fig. 4 that $z/R = 1.113$, which we introduce in the respective equations for the calculation of the third layer, etc. The form of the previous equation for the computing of $S/\pi R^2$ is therefore modified for computing the cross-section of

the r-th layer:

$$\frac{S_j}{\Pi R^2} = \frac{T^2\sqrt{3}}{2\Pi R^2 \rho_{zs}} \sum_{j=1}^{j=r} \gamma_j \, dm_j \qquad (8)$$

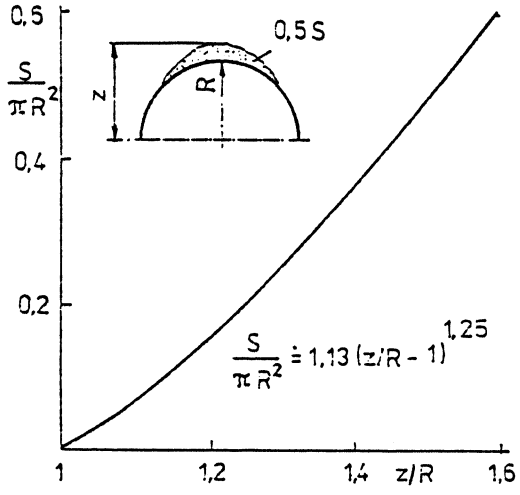

FIGURE 4. Dependence of specific cross-section $S/\Pi R^2$ of the trapped layer on z/R ratio.

This equation assumes that doses dm_j can vary for every layer. With growing the layer of entrapped particles, the force keeping the particles on its surface decreases. For the last (here the tenth) dose, only 28 kg/m^3 are trapped on the rods. The total separated amount is therefore 315 kg/m^3 out of the 500 kg/m^3 brought to the rods. The yield is then $\gamma = 0.63$, recovery $\varepsilon = 0.80$ and Fe content $\beta = 0.32$. The calculation shows that yield, recovery and metal content can be expressed by equations

$$\gamma = \frac{1}{m} \int_0^m dm \int_0^1 \Psi(d_i)\, d\gamma_i$$

$$\varepsilon = \frac{1}{\alpha\, m} \int_0^m dm \int_0^1 \beta_i \Psi\,(d_i)\, d\gamma_i \qquad (9)$$

$$\beta = \alpha\varepsilon/\gamma$$

It is also obvious, from the computing procedure, that double integrals in the first two equations have to be obtained mainly by numerical methods. The computation programme considered also the dependence of flow velocity on the density of suspension. This dependence is different for every type of matrix and can be obtained only experimentally. Fig. 5 illustrates the calculated results of yield, recovery, and metal content obtained under various conditions. All points are seen to lie on two curves, β and ε. Consequently, the metal content and recovery are functions of the yield irrespective of conditions. The same conclusion arises from the basic hypothesis of all models of magnetic separation, which assumes a dynamic equilibrium of attractive and driving forces regardless of conditions under which the equilibrium was attained. Results illustrated in Fig. 5, belong to those outputs of the mathematical model, which inspired us to generalize the results of experimental research of magnetic separation.

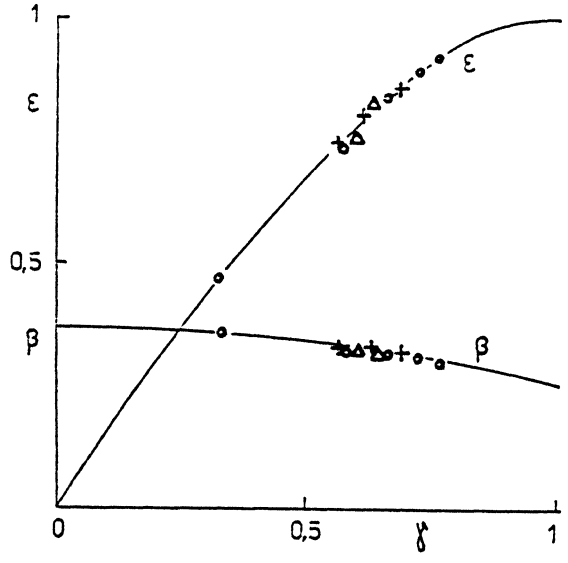

FIGURE 5. Dependence of metal content and recovery on the yield at various 0 - induction, + - velocity, Δ- suspension density.

EQUATIONS OF THE EXPERIMENTAL MODEL

The ouputs of the mathematical model indicated that even the experimentally established values of metal content should prove an analogous dependence on yield as shown in Fig. 5. First, it was necessary to find out the type of dependence involoved and eventually, to construct general equations for functions β and ε. The efforts were finally successful by application of the known experience that every real process is a mere approximation of an ideal one. This involved, in the given case, to define and mathematically express the dependences between the quantities of both the ideal separation and its real approximation.

Ideal separation and its real approximation

As an ideal separation, the separation of a perfectly disintegrated charge into two disjunctive components is considered; in our case it should be an absolutely pure sideroplessite (magnetic component) and the waste rock (gangue) (non-magnetic component). The highest possible yield of concentrate is $\gamma = \alpha/\beta_s$, because at the beginning of an ideal separation absolutely pure sideroplessite represents the concentrate; for given values $\gamma \doteq 1$. At this yield the recovery already equals 1. The dependence of recovery on yield is given by the broken line O-K-A in Fig. 6. The metal content is also illustrated by broken line, β_s-k-α; after point K the metal content decreases according to the hyperbola $\beta = \alpha/\gamma$, because, beginning at this point, the yield cannot be increased but by taking more gangue. The point α reflects the metal content of the feed and it must thus be common to lines β_s -k-α and β_o -α; the former line represents the ideal dependence of metal content on yield while the latter represents the real dependence. The curve illustrating this real dependence starts in point β_o which is always lower than point β_s, because it is not possible during a real separation to prevent some parts of the gangue to be entrained with the magnetic particles of even an ideal feed

(cf. the chapter on limit particle size). The probability, that a non-magnetic particle is followed by a magnetic particle depends on the mass fraction of both kinds of particles. This probability is $P_1 = (\alpha/\beta_s)\ (1-\alpha/\beta_s)$ for an ideal feed. The probability that non-magnetic particles remain entrapped among surrounding particles also depends on the dispersion of these particles in the suspension. For suspensions densities up to $\rho_s \leq 0.3\ \rho_z$, this probability is approximately $P_2 = \rho_s/\rho_{zs}$. Finally, the maximum really attainable metal content of the concentrate can be assessed from

$$\beta_o \doteq \frac{\beta_s}{1 + (\alpha/\beta_s)\ (1-\alpha/\beta_s)\ (\rho_s/\rho_{zs})} \qquad (10)$$

For the tested feed at the given suspension density β_o= 0,3864 may be expected. The distribution of magnetic and non-magnetic particles during ideal and real separation (Fig.6) indicates that the dependence of metal content on yield will be best interpolated by a parabola defined by points β_o, α and tangents at these points. The metal content is then calculated from the equation

$$\beta = \beta_o - (\beta_o-\alpha)\ \gamma^{\alpha/(\beta_o-\alpha)} \qquad (11)$$

The corresponding recovery is computed from the equation (9). The relevant curves β, ε (Fig. 6) are in good agreement with the results of laboratory measurements. Operational measurements are subjected to considerable scattering caused particularly by the variation of metal content of the feed passing through the separator. In some cases this results in quite unrealistic results- see point x in Fig. 6, where the determined recovery of the real concentrate was higher than the recovery obtained by the separation of entirely pure sideroplessite. Lines O-K-A. and β_s -k-α represent namely the limiting theoretically attainable values of metal content and recovery; their significance is comparable with the significance of the Carnot's efficiency for heat engines.

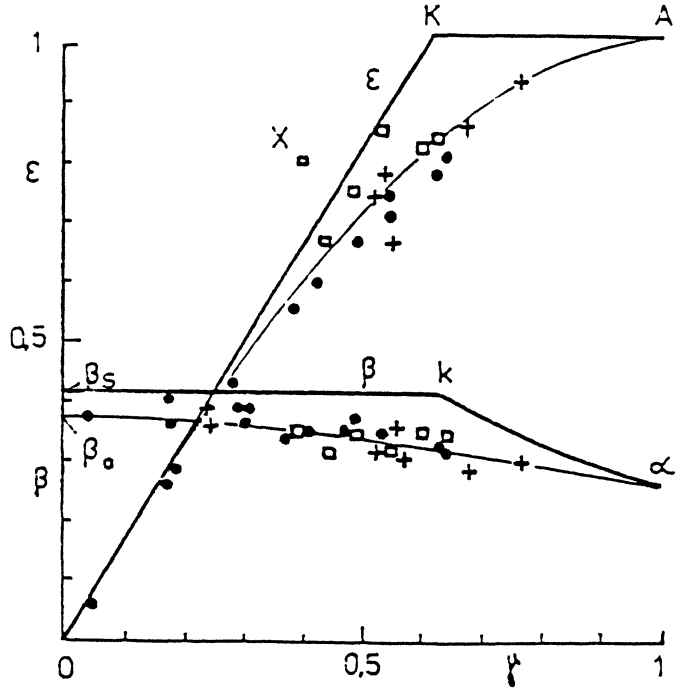

FIGURE 6. Dependence of ε,β, at ideal and real separation 0- laboratory, + - pilot plant, ¤ plant scale.

Acceptably reliable results of operational experiments should be obtained from repeated measurements by statistical methods. The basic aim of operational and laboratory experiments is to determine the yield and metal content of the concentrate under various process conditions. Theoretically, it would be sufficient to determine only the yield and to calculate metal content from the equation (11). For practical purposes it proved better to use a formula in which both assessed quantities γ and β are used. If the yield of γ is expected at different conditions, calculated, for example,from the equation (13), the change of the metal content

β may also be expected according to the formula

$$\beta' = \beta - (\beta_o - \alpha)\left(\gamma'\alpha/(\beta_o - \alpha) - \chi/(\beta_o - \alpha)\right) \qquad (12)$$

The experiments are quite expensive and time-consuming; their number may be reduced considerably by applying the transformation relations of the experimental model. They relate the yield values obtained under various conditions. The equations of the mathematical model can be used to derive that

$$\gamma' = \gamma^J;\ J = \left[\left(\frac{B_o}{B_o}\right)^2 \left(\frac{v'}{v}\right)^{1,4} \left\{\frac{m_o + \gamma' m'}{m_o + \gamma m}\right\}^3\right]^{0.625n} \qquad (13)$$

Here γ is the yield determined at values B_o, v, m; γ' is the yield expected at values B'_o, v', m' if "n" is Rosin-Rammler's exponent for the granulometry of the given feed. Experiments are carried out on the same matrix with same feed; this eliminates the effect of such parameters, which are equal in both experiments and therefore do not occur in the equation (12). Thus, the laboratory experiments are always conducted with matrices with the same arrangement of inductive elements as found in matrices used for industrial separators. The height of laboratory matrices is also the same, only their cross-section is usually smaller. In such a case it should be taken into account that the part of a feed flowing around the matrices walls (and therefore without a separation effect) influences the yield at each matrix to a various extent. The regular arrangement of rods is disturbed near the walls; the rods (indicated in Fig. 1a by dashed lines) are not on the walls and thus particles flowing in the suspension along the walls cannot be trapped. If the width of a matrix in an industrial separator is A', while the width of the matrix in a laboratory experiment is A, the yield obtained in the industrial separator will exceed the laboratory yield by

$$\Delta\gamma, \qquad \Delta\gamma \doteq \frac{T}{2A}\left(1 - \frac{A}{A'}\right) \qquad (14)$$

In addition to that, the suspension in an industrial separator is affected by drifting forces, resulting from the motion of the working element of the separator. The separator is static under laboratory conditions. The influence of the particle-drifting velocity of the working element of the separator on separation results will have to be studied in more detail both experimentally and theoretically.

EXAMPLES

Conversion of laboratory results to industrial-scale conditions

The feed of sideroplessite ore (its properties were already described) was subjected in the laboratory to a high-gradient magnetic separation at magnetic induction of B_o =0.4 T; the suspension density ρ_s = 500 kg/m^3 flowed in the given matrix (width A = 0.04 m) with the velocity of v = 0.14 m/s. The specific matrix load was m = 230 kg/m^3. Under these conditions, the concentrate yield of γ= 0.551 and metal content β = 0.3428 were obtained. Our problem was to establish the yield γ and metal content β' that can be expected in a separator with matrices of width A' = 0.12 m at a higher induction B_o' = 0.5 T. Suspension with a lower density ρ_s = 400 kg/m^3 will flow at a higher velocity v' = 0.15 m/s and the specific separator load will decrease to m'= 210 kg/m^3.

The results of sieve analysis of the feed expressed graphically and numerically (Fig. 3c) were used to establish the Rosin-Ramler's exponent n= 1.5. The value of γ' for the calculation of exponent J in equation (13) must be estimated by approximation. At a higher induction the yield will also be somewhat higher. We estimate γ' = 0.6 then calculate J= 0.718 and $\gamma' = 0.551^{0.7183}$= 0.6517. This more precise value of γ' is used again for computing of J. In the third approximation, a very precise value of the expected yield γ' = 0.6420 is already obtained. We add to it a correction for different matrix widths; it results, from equation (14) that $\Delta\gamma \doteq 0.0375$ and the overall yield of γ' = 0.6795 may be

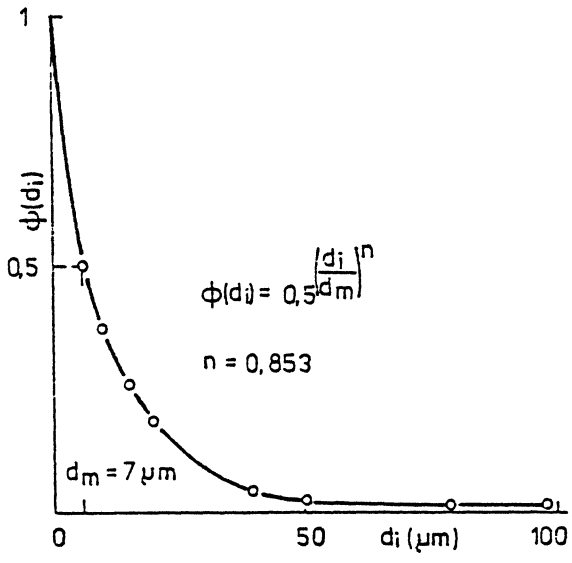

FIGURE 7. Dependence of ψ (d_i) on particle size.

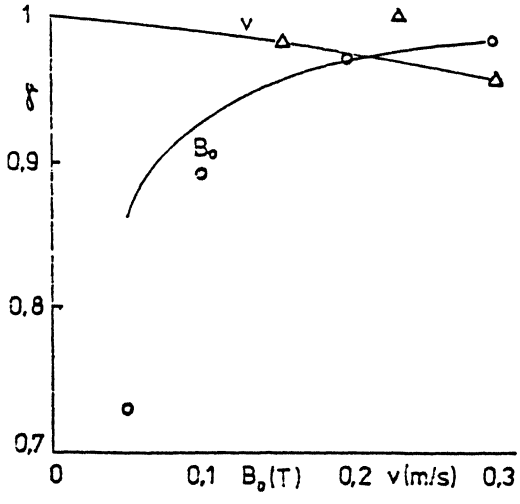

FIGURE 8. The change of the filtration efficiency with induction B_o at v= 0.15 m/s and velocity v at B_o= 0.3 T.

expected. If we introduce into equation (12) the already known values of $\alpha = 0.2517$ and $\beta_o = 0.3864$ we can compute that the metal content should be $\beta' = 0.3216$, A comparison of computed and experimentally obtained results is shown in the following table:

	γ'	β'	ε'
Conversion results	0.6795	0.3216	0.8682
Experimental results	0.6450	0.3351	0.8587
Difference	3.45%	-1.35%	0.95%

Mathematical formulation of experimental results

The equations of both models can be conveniently used for mathematical formulation of experimentally determined relationships. Table 1 presents experimental results of magnetic filtration of a steel-plant effluent polluted by magnetite of the grain size shown in Fig.7.

The graphical illustration of these results (Fig. 8) indicates that their expression by means of regression methods would be very disadvantageous. In addition to that, the regression expression of a function of two variable $\gamma = f(B_o, v)$ would also require many additional measurements. The relative amount of particles trapped in a filtration matrix is called filtration effectiveness, this being only a better term for the yield γ. If only B_o, v change during the experiments, it is possible to sum up the effects of other quantities into a single constant K. Similarly, as for the equation (13), the expression for filtration effectiveness can be found

$$\gamma = 0.5^{K\,(v^{1.4}/\,B_o^{\,2}\,)^{0.625n}}$$

TABLE I Results of experimental magnetic filtration

Measurement No.	B_o (T)	v (m/s)	γ
1.	0.05	0.15	0.730
2.	0.10	0.15	0.830
3.	0.20	0.15	0.975
4.	0.30	0.15	0.984
5.	0.30	0.19	0.988
6.	0.30	0.24	0.957

Measurement results quoted in Table 1 are used to determine the mean value of K = 0.033. It may be seen, in the Fig. 8, that the calculated dependences B_o, v, are very close to experimental results. The application of model equations simplified the otherwise very laborious regression analysis to the determination of one single constant.

CONCLUSION

As stated in an editorial note in Magnetic Separation News[4], many experts from industrial establishments point out a discrepency between current theoretical models and their excessively idealized interpretation on the one hand, and actual plant scale results on the other. Many of these disproportions were stressed also by Svoboda[5] (ibid).

Here we attempted to combine two approaches in order to solve this problem both theoretically and experimentally. We derived equations for both the mathematical and experimental models incorporating the majority of the known theoretical and experimental parameters, which affect the process of high-gradient magnetic separation. Mathematical modelling, complemented by some experimentally determined values, enabled the process parameters, to be determined even for industrial-scale conditions, with a high reliability. The results were checked and verified in plant-scale

conditions during the HGM separation of a sideroplessite ore from Rudnany on VMS separators[6]. All data hold for oriented rod matrices (cf. Fig.1) used in Czechoslovak HGM separators of the type VMS. However, it can be expected that they are applicable to other types of matrices used in other countries. The main advantage of the model is that it permits a substantial reduction of experimental work and thus eliminates one most crucial obstacle in the wider expansion of the HGMS process. Apart from the high cost of HGM separators, the necessity of extensive laboratory, pilot-plant model, and plant-scale investigation and verification together with the determination of optimum separation conditions for individual specific raw materials constituted hitherto the main drawback of the HGMS process.

REFERENCES

1. V. Hencl, K. Jahoda, E. Madai, Magnetic Sep. News, 1, 173-182 1985.
2. P. Mucha, V. Hencl. E. Madai. Inter. Jour. of Min. Process., 9, 259-268 1982.
3. K. Johoda, Elektrotech. Obzor, 3, 159-162, 1984.
4. Anon, Magnetic Sep. News, 2, 49 1986.
5. J. Svoboda, Magnetic Sep. New, 2, 51-68- 1986.
6. V. Hencl, G. Sebor, Proc: XVth INTERNATIONAL MINERAL PROCESSING CONGRESS, Cannes, France, June 1985, Tom 1. 354-362.